

# UWB Monocycle Generator Based on the Non-Linear Effects of an SOA-Integrated Structure

Vanessa Moreno, Manuel Rius, Jose Mora, Miguel A. Muriel  
and Jose Capmany

**Abstract**—In this letter, we propose and experimentally demonstrate a novel and single structure to generate ultra-wideband (UWB) pulses by means of the cross-phase modulation present in a semiconductor optical amplifier unified structure. The key components of this system is an integrated Mach-Zehnder interferometer with two semiconductor optical amplifiers and an optical processing unit. The fusion of these two components permits the generation and customization of UWB monocycle pulses. The polarity of the output pulses is easily modified through the single selection of a specific input port. Moreover, the capacity of transmitting several data sequences is demonstrated and the potentiality to adapt the system to different modulation formats is analyzed.

**Index Terms**—Microwave photonics, optical interferometry, semiconductor optical amplifiers, ultra wideband technology, optical communications.

## I. INTRODUCTION

ULTRA-WIDE band (UWB) technology has been a topic of interest in the fields of short range communications, high-capacity wireless and broadband sensor networks for quite some time [1]. UWB signals have attracted much interest because of their potential to transmit high data rates, low power consumption, immunity to multipath fading, interference mitigation, low loss, carrier free and especially because of their capacity of sharing their corresponding spectrum with other narrowband technologies.

Parallel to the increasing use of UWB technology, there has been a considerable interest in the implementation of photonic solutions in order to profit from the benefits of Microwave Photonics (MWP) [2]. For instance, the range of distance of an UWB scheme can be increased through the distribution of the UWB signals in the optical domain or UWB over fiber

(UWBoF) [3]–[5]. The application of MWP is not limited to the distribution process but this technology is also employed for UWB signal generation processing and control. The inherent advantages of the optical domain such as low losses, lightweight, high bandwidth, tunability, reconfigurability and immunity to electromagnetic interference show the generation in the optical domain as an attractive and practical approach without needing any extra electrical-optical conversion.

In principle, high order pulses feature a better performance in UWB communication systems as they comply with the US FCC mask [6]. However, monocycle and doublets are pulses widely used in UWB systems due because they offer other advantages related to multipath performance and simplicity [7] offering a potential integration [8].

In this context, UWB pulse generation techniques in the optical domain have been proposed and can be classified into methods based on phase modulation to intensity modulation (PM-IM) [9], optical spectral shaping and dispersion-induced frequency-to-time mapping [10], microwave photonic filtering [11] and semiconductor optical amplifiers [12]–[14]. The employment of SOAs appears as an attractive due to its nonlinear effects, low power consumption, flexibility, scalability and the potential of chip integration. In [12], a monocycle or a doublet are obtained through an all-optical implementation based on SOA-XPM effect and DWDM-based multi-channel frequency discriminator. In [13], a pair of polarity-reversed UWB monocycle pulses are generated and modulated with Bi-Phase modulation format by applying non-return-to-zero (NRZ) data to the radio frequency port of a Mach-Zehnder (MZ) Modulator. Finally, a theoretical analysis of the integration of XPM and XGM in a nonsymmetrical MZ interferometer (MZI) concludes with the feasibility of generating IR-UWB doublets [14].

In this letter, a novel scheme for generation of an UWB monocycle and data transmission is proposed and experimentally demonstrated. This approach exploits the properties of a MZI, which is composed of two semiconductor optical amplifiers (SOAs) with the reconfiguration capabilities provided by an additional an optical processor unit. Two continuous wave probe signals and a pump signal are employed in order to induce cross-phase modulation (XPM) in the SOA-MZI structure. It is feasible to modify the system output pulse polarity by introducing the previously mentioned inputs with a specific wavelength through a particular input port. This solution is potentially scalable to obtain high order pulses by introducing additional optical taps. In addition to

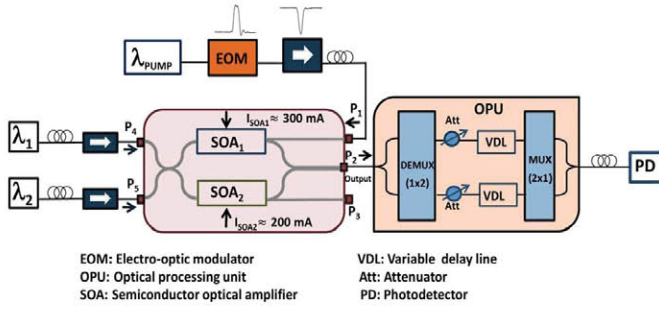


Fig. 1. Experimental design for UWB signal generation and customization.

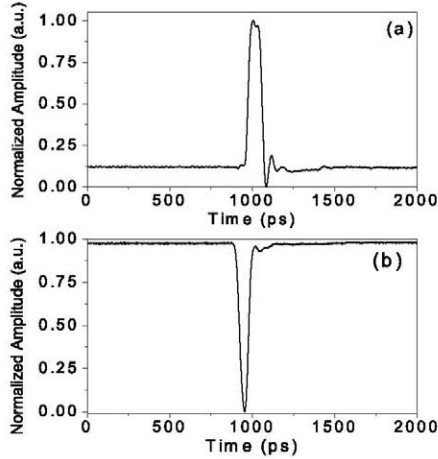


Fig. 2. (a) Electrical input pulsed signal prior to the EOM and (b) modulated optical pulse employed as pump signal.

the generation process, the modulation of monocycle pulses is also proposed.

## II. PRINCIPLE OF OPERATION

Fig. 1 depicts the proposed design for generation and customization of an UWB monocycle. It corresponds to a microwave photonic filter composed of a SOA-MZI and an optical processor unit. The SOA-MZI consists of an interferometric structure that contains a pair of InGaAsP SOAs with low polarization sensitivity, one in each branch of the MZI. Both cross-gain modulation (XGM) and cross-phase modulation (XPM) effects could be present in the SOAs. However, the linewidth enhancement factor of these devices is large enough to neglect the XGM effect [15], [16].

The scheme is fed by a pump signal centered at an optical wavelength  $\lambda_{\text{PUMP}} = 1535.04\text{nm}$  and two continuous probe signals (labeled as  $\lambda_1$  and  $\lambda_2$ ) centered at 1550.12 nm and 1552.52 nm, respectively. The bit sequence corresponding to the pump signal is set with a pattern of one “1” and sixty-three “0”, summing up a total of 64 bits, at a repetition rate of 12.5 GHz. The optical power related to this source is 5.29 dBm. The obtained waveform after the modulation stage (EOM) corresponds to an inverted Gaussian pulse when compared to the original pump signal. Both the input pulse and the modulated optical carrier are represented in Fig. 2(a) and (b) respectively.

As shown in Fig. 1, each optical signal is introduced independently to the SOA-MZI by different ports. In particular,

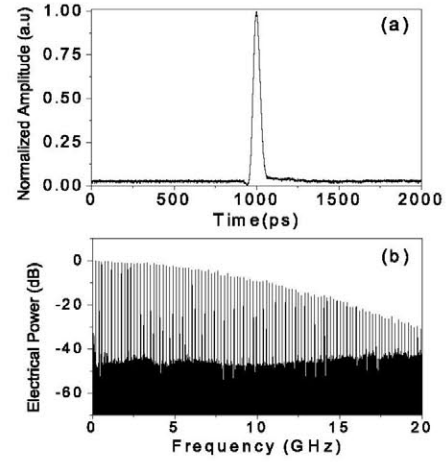


Fig. 3. (a) Positive tap pulse generated and (b) corresponding electrical spectrum.

the pump signal is launched into port  $P_1$  and each probe signal ( $\lambda_1$  and  $\lambda_2$ ) is launched into a different port ( $P_4$  or  $P_5$ ). Therefore, this architecture employs a counter-propagation configuration. Indeed, no optical filter is needed to separate the pump signal from the probe signals  $\lambda_1$  or  $\lambda_2$ .

In order to show the principle of operation, we introduced into port  $P_4$  the optical wavelength  $\lambda_1$  at 1550.12 nm as a probe signal. As it was above mentioned, the modulated pulse acting as pump signal is launched into the SOA-MZI through the port  $P_1$  and the output generated pulse is measured at port  $P_2$ . Fig. 3(a) and (b) display the obtained pulse and the corresponding spectrum, respectively. We can observe that a positive pulse is generated, which is inverted in accordance with the pump signal of Fig. 2(b).

The most important optical and electrical parameters of the SOA-MZI are the current applied to each SOA and the optical power related to the input optical signals (pump and probes). The upper branch of the SOA-MZI contains the SOA1 with a high constant current of 300 mA that determines the speed conversion of the continuous input signal. In this way, the conversion efficiency or the gain depends on the current injected to SOA2 with a threshold current around 40 mA. Different maximum conversion points are located at current applied to SOA2 close to 150 mA and 300 mA whereas the minimum conversion one is close to 240 mA. As shown in [15], we observe that the polarity of the generated pulse is established by the operation current point to perform the wavelength conversion. The relative phase between the output and input signal changes from  $0^\circ$  to  $180^\circ$  for different regions and, in particular, for operation points located at the maximum conversion zone. Therefore, the influence of the bias current on the SOA gain and the conversion process determines the operation current of SOA2 around 200 mA obtaining a positive pulse and negative pulse at the output port  $P_2$  depending on the input port  $P_4$  and  $P_5$ , respectively.

For this experimental setup, the polarity is determined by the interferometric structure. It is possible to achieve a positive or negative pulse by selecting the adequate input port. Fig. 4(a) and (b) display the optical pulse and the corresponding electrical spectrum when the probe signal is

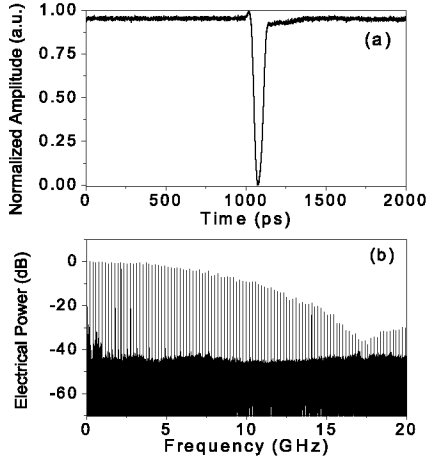


Fig. 4. (a) Negative tap pulse generated and (b) corresponding electrical spectrum.

launched into port P<sub>5</sub>. The optical power value employed was 4.44 dBm. Comparing with Fig. 3, a polarity inversion is observed due to the selected input port. In this case, a negative optical pulse is generated.

Taking into account these previous results, the generation of monocycle pulses can be obtained as a result of the combination of these positive and negative tap pulses generated by means of the port P<sub>4</sub> and P<sub>5</sub>, respectively.

The functionality of the OPU consists on the control of the amplitude and delay parameters for each generated optical pulse. The generation process requires a reconfiguration of the pulses obtained previously to the OPU independently from their polarity. Therefore, OPU is the key element to provide flexibility in the system in terms of reconfiguration capability. In this case, this assembly is composed of the concatenation of two demultiplexing stages. All generated signals coming from the port P<sub>2</sub> of the SOA-MZI are introduced into a  $1 \times 2$  demultiplexing device. Every signal pulse carried at a different optical wavelength is treated independently. Each one is customized in terms of amplitude and delay by means of attenuators and variable delay lines. Finally, the output signal is obtained by combining all processed optical pulses through a  $2 \times 1$  multiplexing device which output port permits us to visualize the accomplished monocycle through a photodetector (PD).

### III. EXPERIMENTAL RESULTS

As it has been demonstrated in the prior section, the proposed system has the ability of generating both positive and negative tap pulses. The combination and reconfiguration of these optical pulses through the optical processing unit permits to generate an UWB monocycle pulse as shown in Fig. 5. Time-domain waveforms have been measured with a sampling oscilloscope without averaging.

In Fig. 5(a), we have plotted a waveform which is generated by means of two laser sources centered at optical wavelengths  $\lambda_1$  and  $\lambda_2$ ; they are launched into ports P<sub>4</sub> and P<sub>5</sub>, respectively. As shown, this waveform is composed by two Gaussian pulses with inverse polarities and a time separation of 440 ps approximately. Fig. 5(b) depicts their corresponding spectral

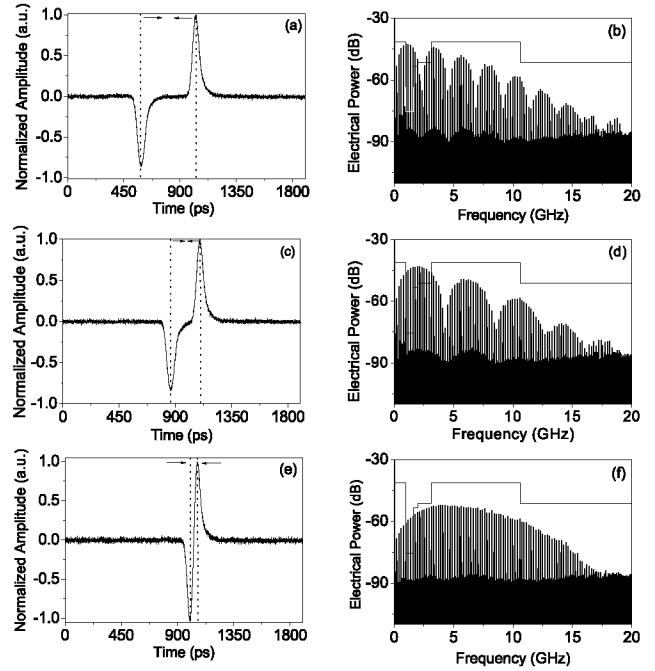


Fig. 5. (a) Generated pulses in their original position, prior to the delay configuration, (b) corresponding spectral representation, (c) generated pulses with a 200 picoseconds approximation, (d) spectral representation for the modified pulses, (e) obtained monocycle waveform after final delay configuration and (f) spectrum for the obtained UWB monocycle pulse.

representation, which is far from resembling the desired UWB monocycle. In this case, the first maximum of the spectrum is close to GPS band (0.9 GHz–1.61 GHz) since the Free Spectral Range (FSR) is around 2.2 GHz ( $FSR \approx 1/\tau$ ). In order to achieve a better fit, in Fig. 5(c) we reduce the time distance between these two signals through the variable delay lines that composed the optical processing unit. In this case, the optical delay between optical taps is close to 240 ps implying a modification of the FSR (4.2 GHz) as can be appreciated in Fig. 5(d). We observe that first maximum is displaced to higher frequencies up to 2.1 GHz.

Finally, the separation between the positive and negative pulse is reduced to an optimized value close to 60 ps as shown in Fig. 5(e). When analyzing the corresponding spectrum of the generated pulse, which is depicted in Fig. 5(f), we observe that this waveform reveals a better adjustment in terms of fitting the FCC spectral mask parameters. In this case, the FSR is 16.7 GHz approximately which is compatible with the UWB mask. Even though monocycles do not fully satisfy successfully the FCC spectral mask restriction as predicted theoretically [6], they provide remarkable advantages in terms of achievability, simplicity and integration [7], [8].

The proposed scheme can be used to perform data transmission by means of the generated UWB monocycle pulses. As previously shown, our approach is based on the combination of two complementary positive and negative pulses providing an UWB monocycle pulse. It is plausible to transmit a data sequence Pulse Amplitude Modulation (PAM) by modifying the bit sequence of the pump signal. Fig. 6 plots the transmission of three different data sequences and

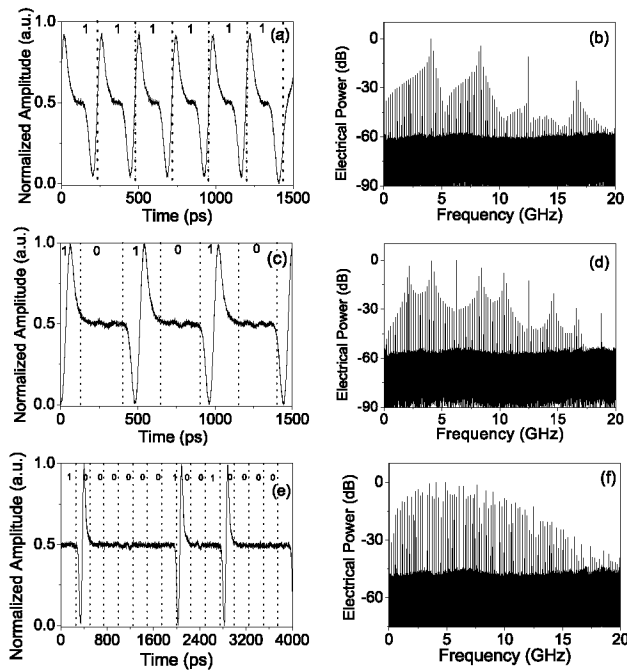


Fig. 6. (a) First data scheme transmitted with a bit sequence of all ones “1” and (b) corresponding spectral representation. (c) Second data series composed of both ones “1” and zeros “0” bits and (d) respective spectrum. (e) Third data sequence transmitted and (f) electrical spectrum.

the corresponding spectra. First data scheme was transmitted with a bit sequence of all ones “1” and second data series was composed of both alternated ones “1” and zeros “0” bits as shown in Fig. 6(a) and (b), respectively. A third data sequence was transmitted with “0” and “1” distributed randomly as plotted in Fig. 6(c). Moreover, Fig. 6(b), (d), and (f) depict the corresponding spectra.

Alternatively, PAM can be also implemented by means of variable optical attenuators that provide the amplitude of each optical pulse. Also, Pulse Position Modulation (PPM) can be achieved by controlling the relative position of pulses in the time domain by means of each optical variable delay line. Finally, Bi-Phase Modulation (BPM) can be also easily implemented by adding an optical switch prior to the conversion stage (SOA-MZI). We could automatically change the polarity of the obtained signal and therefore achieve two complementary monocycle pulses. On the other hand, our approach can be extended to generate high order pulses increasing the number of optical taps. In this case, Pulse Shape Modulation (PSM) can be also implemented by means of the delay and amplitude in the optical processor unit.

#### IV. CONCLUSION

A novel approach to generate an UWB monocycle has been proposed and experimentally demonstrated based on the combination of Gaussian positive and negative pulses.

The polarity of the pulses is carried out by exploiting the XPM effect present in an interferometric structure. Moreover, the reconfiguration of the pulses is achieved by means of an optical processor unit which permits to control the amplitude and time delay of each optical pulse. The scalability of the system is potentially attractive to obtain higher order pulses by introducing additional optical probe signals and adapting the optical processing unit. Finally, data transmission has been also accomplished through various sequences transmitted and a potential adaptation to different format modulations has been analyzed.

#### REFERENCES

- [1] J. Yao, “Photonics for ultrawideband communications,” *IEEE Microw. Mag.*, vol. 10, no. 4, pp. 82–95, Jun. 2009.
- [2] J. Capmany and D. Novak, “Microwave photonic combines worlds,” *Nature Photon.*, vol. 1, no. 6, pp. 319–330, Jun. 2007.
- [3] Y. Le Guennec, M. Lourdiane, B. Cabon, G. Ghislaine, and P. Lombard, “Technologies for UWB-over-fiber,” in *Proc. Annu. Meeting IEEE Lasers Electro Opt. Soc.*, Oct. 2006, pp. 518–519.
- [4] S. Pan and Y. Yao, “UWB-over fiber communications: Modulation and transmission,” *J. Lightw. Technol.*, vol. 28, no. 16, pp. 2445–2455, Aug. 15, 2010.
- [5] P. Li, S. Wang, H. Chen, M. Chen, and S. Xie, “Photonic generation of various modulation formats in high speed UWB over fiber system,” in *Proc. IEEE Topical MWP*, Oct. 2010, pp. 309–312.
- [6] H. Sheng, P. Orlik, A. Haimovich, L. Cimini, and J. Zhang, “On the spectral and power requirements for ultra-wideband transmission,” in *Proc. IEEE Int. Conf. Commun.*, May 2003, pp. 738–742.
- [7] Q. T. Le, D. Briggmann, and F. Kueppers, “Generation of UWB pulses using direct modulation of semiconductor laser and optical filtering,” *Electron. Lett.*, vol. 49, no. 18, pp. 1171–1173, Aug. 2013.
- [8] X. Xu, C. Zhenzhou, Y. W. Wong, and K. T. Hon, “UWB monocycle pulse generation based on colourless silicon photonic integrated circuit,” *Electron. Lett.*, vol. 49, no. 20, pp. 1291–1293, Sep. 2013.
- [9] F. Zeng and J. Yao, “Ultrawideband impulse radio signal generation using a high-speed electrooptic phase modulator and a Fiber-Bragg-Grating-based frequency discriminator,” *IEEE Photon. Technol. Lett.*, vol. 18, no. 19, pp. 2062–2064, Oct. 1, 2006.
- [10] M. Abathi, M. Mirshafiei, J. Magné, L. A. Rusch, and S. LaRochelle, “Ultra-wideband waveform generator based on optical pulse-shaping and FBG tuning,” *IEEE Photon. Technol. Lett.*, vol. 20, no. 2, pp. 135–137, Jan. 15, 2008.
- [11] M. Bolea, J. Mora, B. Ortega, and J. Capmany, “Optical UWB pulse generator using an N tap microwave photonic filter and phase inversion adaptable to different pulse modulation formats,” *Opt. Express*, vol. 17, no. 7, pp. 5023–5032, Mar. 2009.
- [12] Y. Yu, J. Dong, X. Li, and X. Zhang, “UWB monocycle generation and bi-phase modulation based on Mach-Zehnder modulator and semiconductor optical amplifier,” *IEEE Photon. J.*, vol. 4, no. 2, pp. 327–339, Apr. 2012.
- [13] X. Zhang, E. Xu, and Y. Zhang, “All-optical UWB generation and modulation for multiuser UWB-over-fiber system,” in *Proc. Asia Commun. Photon. Conf. Exhibit.*, Dec. 2010, pp. 168–169.
- [14] M. Ran, B. I. Lembrikov, and Y. Ben Ezra, “Ultra-wideband radio-over-optical fiber concepts, technologies and applications,” *IEEE Photon. J.*, vol. 2, no. 1, pp. 36–48, Feb. 2010.
- [15] M. D. Manzanedo, J. Mora, and J. Capmany, “Continuously tunable microwave photonic filter with negative coefficients using cross-phase modulation in an SOA-MZ interferometer,” *IEEE Photon. Technol. Lett.*, vol. 20, no. 7, pp. 526–528, Apr. 1, 2008.
- [16] G. P. Agrawal and N. A. Olsson, “Self-phase modulation and spectral broadening of optical pulses in semiconductor laser amplifiers,” *IEEE J. Quantum Electron.*, vol. 25, no. 11, pp. 2297–2306, Nov. 1989.